ZKG INTERNATIONAL

ISSN: 2366-1313

THREE-DIMENSIONAL ROTATING SURFACE WITH THERMOPHORESIS AND VARIABLE THERMAL CONDUCTIVITY IN MAXWELL NANOFLUID

Lakshmi R[1], Kanchana M[1*]
[1]PSGR Krishnammal College for Women, India

Abstract: Bidirectional stretching sheet with thermophoresis velocity and variable thermal conductivity investigated in Maxwell nanofluid due to rotating frame. Cattaneo-Christov model (CC-model) introduced in thermal and solute field. Double stratification is applied over heat and mass transfer. The system of partial differential equation is transformed into ordinary boundary value problem by using suitable transformation. This model is solved through bvp4c Matlab solver numerically and graphically. Moreover, Magnetite nanoparticle with base fluid water occurs and shape factor causes nanoparticle to produce its effects over thermal field. Larger elasticity reduces the fluid velocities. Collision of nanoparticle causes temperature strengthens and improves thermal conductivity. The numerical solutions are compared with previously published papers and this comparison made well-being results.

KEYWORDS: Maxwell nanofluid, Rotating, CC-Model, variable thermal conductivity, thermophoresis.

1. INTRODUCTION

Many unique attempts have been documented by researchers in the last century as a result of motivated the uses of nanofluids in industrial and technological processes. A plethora of nanofluid communications have been tackled in the last decade due to advancing thermal effect. The nanomaterial are made up of metallic particles suspended in water based fluid. The fascinating uses of nanomaterial include heat exchangers, solar systems, hybrid-powered engines, micro-electronics, thermal management ad so on. The nanofluids are a period of sequential thermal propagated liquid prepared by dispersing small-scale nanoparticles across the width of a convectional heat transmitted liquid. Nanoparticles are commonly used in the freezing of atomic activators, cancer treatment and medication cycles. Bonyah et al. [4] discussed the flow model which is combination of variable thermal conductivity and nanoparticle motion effects with physical behaviour of sphere on the flow of natural convection for various values of parameters and they illustrated through graphical and numerical purpose.

Nainaru Tarakaramu et al. [16] studied and solved the problem of three dimensional steady flow of radiation and variable conductivity of magneto hydrodynamics nanofluid by a stretched surface numerically and graphically. A non-isothermal surface of porous medium with steady flow under thermal conductivity examined and calculated by analytically through perturbation technique over the graphical illustrations by S.A.Shehzad et al. [14]. The non-linear problem of laminar flow is discussed by M. Mustafa et al. [10]. Then at wall, analytical solution for the missing tangential surface are solved with HAM technique for wide range of parameters. The coaxial rotating disks are stretched in three dimensional flow with magnetic field and analysed the velocity, concentration and temperature profiles by exact solution in a graphical and tabulated form by Muhammed Altaf Khan et al. [2]. Boungiorno theory of nanofluid, CC-model, thermal conductivity are analysed with stefan blowing effects and mass convection in a gyrating disk at the wall. Rauf [9] solved this problem by numerically. The gyrostatic motile organisms, CC-heat flux model used simultaneously with variable thermal conductivity and temperature dependant viscosity in nanoliquid across a rotating disk on effects of chemical reaction and non-uniform source/sink by Muhammad Ramzan [12]. In a rotational frame, three dimensional steady flow of nanoliquid with partial slip and magnetic strength using different shapes and diameter of nanoparticles are illustrated by Aziz Ullah Awan et al. [3]. This problem portrayed through graphs and tables on comparative results with previous research work.

ISSN: 2366-1313

Karem Mahmoud Ewis et al. [6] studied the viscoelastic fluids between vertical plates with the influence of Grashof number and thermal conductivity on non-Darcian convectional flow. Previous work is compared with numerical values which is calculated by iteration methods with linearization technique. In a rotating system, thermal convective boundary layer flow is investigated across a vertical plate and R. Bhuvanavijaya et al. [5] explored heat and mass transfer, chemical reaction, porosity and conductivity which are all calculated through RK-method with shooting procedure. The non-linear problem is solved through Galerkin method. J. A. Gbadeyan et al. [7] investigated magnetic casson nanoliquid across a vertical plate with combined effects of radiation, conductivity, viscosity and non-Darcian porosity. In a wavy surface, Bandaru Mallikarjuna et al. [15] described the transport phenomena of thermophoresis on convective condition with variable properties. Heat generation, thermal conductivity and temperature dependant viscosity are assumed by G. C. Hazarika et al. [8] along a vertical porous plate. Then this problem examined through graphically and numerically. The transfer rate of heat and mass also identified through thermal and solute profiles. With variable thermal conductivity, heat generation and thermophoresis in an isothermal moving surface is radiated by M.G. Reddy [13] across a semi-infinite plate under free convective boundary condition. Ahmad et al. [1] CC-model with double stratification in Maxwell fluid across stretched sheet explored and analysed the transfer rate of heat and mass by numerically through bvp4c Matlab technique. The tabulated values of velocity gradient are compared with previous work. In an isothermal horizontal porous plate, two-dimensional surface in micro polar fluid with Darcy, thermophoresis and conductivity effects are modelled and framed the problem to find the numerical values and graphs are illustrated by Hossam A. Nabwey et al. [11] through Matlab technique.

Based on review of literature, the study comes down to the fluid flow of various surface with variable thermal conductivity, thermophoresis, CC-model, double stratification and Maxwell condition. With nanofluid properties, different shape factors and diameter of nanoparticles occurred but bidirectional stretching surface due to rotating frame is considered in this present work to challenges the results of velocity compared previous articles, heat and mass transfer also analysed. And the problem is solved numerically and graphically through bvp4c Matlab technique. The thickness of boundary layer also portrayed through graphical form.

2. MATHEMATICAL DEMONSTRATION

Examine the bidirectional rotating surface with steady, incompressible, three dimensional metal sheet in Maxwell nanofluid (Magnetite-water/ Fe_3O_4-H_2O). The secondary fluid motion occurs in z-direction with constant angular velocity ω due to Coriolis force. The velocity of fluid flow are u_1, v_1 and w_1 in the x, y and z-directions respectively. The velocities at the wall $u_1 = a_1x$(x-direction) and $v_1 = a_2y$ (y-direction), where a_1 and a_2 are positive real numbers. With the use of CC model, the equation of energy is updated to simulate thermal and solute impacts with double stratification, variable thermal conductivity and thermophoresis effects. The temperature denoted as T_w and T_∞ and concentration C_w and C_∞ at surface and ambient respectively.

$$\frac{\partial u_1}{\partial x}+\frac{\partial v_1}{\partial y}+\frac{\partial w_1}{\partial z}=0 \tag{1}$$

$$\begin{aligned}
&u_1\frac{\partial u_1}{\partial x}+v_1\frac{\partial u_1}{\partial y}+w_1\frac{\partial u_1}{\partial z}-2\omega v_1=\frac{\mu_{nf}}{\rho_{nf}}\frac{\partial^2 u_1}{\partial z^2}\\
&-\lambda_1\Bigg[u_1^2\frac{\partial^2 u_1}{\partial x^2}+v_1^2\frac{\partial^2 u_1}{\partial y^2}+w_1^2\frac{\partial^2 u_1}{\partial z^2}+2u_1v_1\frac{\partial^2 u_1}{\partial x\partial y}\\
&+2v_1w_1\frac{\partial^2 u_1}{\partial y\partial z}+2u_1w_1\frac{\partial^2 u_1}{\partial x\partial z}-2\omega\Bigg(u_1\frac{\partial v_1}{\partial x}\\
&+v_1\frac{\partial v_1}{\partial y}+w_1\frac{\partial v_1}{\partial z}\Bigg)+2\omega\Bigg(v_1\frac{\partial u_1}{\partial x}-u_1\frac{\partial u_1}{\partial y}\Bigg)\Bigg]\\
&-\frac{\sigma_{nf}B_0^2}{\rho_{nf}}\Bigg(u_1+\lambda_1w_1\frac{\partial u_1}{\partial z}\Bigg)
\end{aligned} \tag{2}$$

$$\begin{aligned}
&u_1\frac{\partial v_1}{\partial x}+v_1\frac{\partial v_1}{\partial y}+w_1\frac{\partial v_1}{\partial z}+2\omega u_1=\frac{\mu_{nf}}{\rho_{nf}}\frac{\partial^2 v_1}{\partial z^2}\\
&-\lambda_1\Bigg[u_1^2\frac{\partial^2 v_1}{\partial x^2}+v_1^2\frac{\partial^2 v_1}{\partial y^2}+w_1^2\frac{\partial^2 v_1}{\partial z^2}+2u_1v_1\frac{\partial^2 v_1}{\partial x\partial y}\\
&+2v_1w_1\frac{\partial^2 v_1}{\partial y\partial z}+2u_1w_1\frac{\partial^2 v_1}{\partial x\partial z}-2\omega\Bigg(u_1\frac{\partial u_1}{\partial x}\\
&+v_1\frac{\partial u_1}{\partial y}+w_1\frac{\partial u_1}{\partial z}\Bigg)+2\omega\Bigg(v_1\frac{\partial v_1}{\partial x}-u_1\frac{\partial v_1}{\partial y}\Bigg)\Bigg]
\end{aligned}$$

ISSN: 2366-1313

$$-\frac{\sigma_{nf}B_0^2}{\rho_{nf}}\left(v_1+\lambda_1 w_1\frac{\partial v_1}{\partial z}\right) \quad (3)$$

$$u_1\frac{\partial T}{\partial x}+v_1\frac{\partial T}{\partial y}+w_1\frac{\partial T}{\partial z}=\frac{1}{(\rho c_p)_{nf}}\frac{\partial}{\partial z}\left(k(T)\frac{\partial T}{\partial z}\right)$$
$$+\frac{H_0}{(\rho c_p)_{nf}}(T-T_\infty)-\lambda_2\left[u_1^2\frac{\partial^2 T}{\partial x^2}+v_1^2\frac{\partial^2 T}{\partial y^2}+w_1^2\frac{\partial^2 T}{\partial z^2}\right.$$
$$+2u_1v_1\frac{\partial^2 T}{\partial x\partial y}+2v_1w_1\frac{\partial^2 T}{\partial y\partial z}+2u_1w_1\frac{\partial^2 T}{\partial x\partial z}+\left(u_1\frac{\partial u_1}{\partial x}\right.$$
$$\left.+v_1\frac{\partial u_1}{\partial y}+w_1\frac{\partial u_1}{\partial z}\right)\frac{\partial T}{\partial x}+\left(u_1\frac{\partial v_1}{\partial x}+v_1\frac{\partial v_1}{\partial y}+w_1\frac{\partial v_1}{\partial z}\right)\frac{\partial T}{\partial y}$$
$$\left.+\left(u_1\frac{\partial w_1}{\partial x}+v_1\frac{\partial w_1}{\partial y}+w_1\frac{\partial w_1}{\partial z}\right)\frac{\partial T}{\partial z}\right] \quad (4)$$

$$u_1\frac{\partial C}{\partial x}+v_1\frac{\partial C}{\partial y}+w_1\frac{\partial C}{\partial z}=D\frac{\partial^2 C}{\partial z^2}-\frac{\partial}{\partial z}(V(T)(C-C_\infty))$$
$$+\Gamma(C-C_\infty)-\lambda_3\left[u_1^2\frac{\partial^2 C}{\partial x^2}+v_1^2\frac{\partial^2 C}{\partial y^2}+w_1^2\frac{\partial^2 C}{\partial z^2}\right.$$
$$+2u_1v_1\frac{\partial^2 C}{\partial x\partial y}+2v_1w_1\frac{\partial^2 C}{\partial y\partial z}+2u_1w_1\frac{\partial^2 C}{\partial x\partial z}+\left(u_1\frac{\partial u_1}{\partial x}\right.$$
$$\left.+v_1\frac{\partial u_1}{\partial y}+w_1\frac{\partial u_1}{\partial z}\right)\frac{\partial C}{\partial x}+\left(u_1\frac{\partial v_1}{\partial x}+v_1\frac{\partial v_1}{\partial y}+w_1\frac{\partial v_1}{\partial z}\right)\frac{\partial C}{\partial y}$$
$$\left.+\left(u_1\frac{\partial w_1}{\partial x}+v_1\frac{\partial w_1}{\partial y}+w_1\frac{\partial w_1}{\partial z}\right)\frac{\partial C}{\partial z}\right] \quad (5)$$

with associated boundary conditions,

$$\begin{aligned}&\text{At } z=0, u_1=a_1x, v_1=a_2y, w_1=0,\\ &T_w=T=d_1x+T_0, C_w=C=d_2x+C_0\\ &\text{As } z\to\infty, u_1\to 0, v_1\to 0, T\to T_\infty=e_1x+T_0,\\ &C\to C_\infty=e_2x+C_0\end{aligned} \quad (6)$$

Table 1. Thermophysical properties of nanofluid.

Properties	ρ (kg/m^3)	C_p ($J/kg\,K$)	k ($W/m\,K$)	σ (S/m)
Water	997.1	4179	0.613	5.5×10^6
Copper	8933	385	401	59.6×10^6
Alumina	3970	765	40	35×10^6
Magnetite	5180	670	9.7	0.74×10^5

Here, variable thermal conductvity and thermophoretic velocity,

$$k(T)=k_\infty\left(1+\varepsilon\left(\frac{T-T_\infty}{T_w-T_0}\right)\right),\quad V(T)=-\upsilon_{bf}\frac{k^*}{T_r}\frac{\partial T}{\partial z} \quad (7)$$

Thermophysical properties for Maxwell Nanofluid :

$$\mu_{nf}=\frac{\mu_{bf}}{(1-\phi)^{2.5}},\ (\rho c_p)_{nf}=(1-\phi)(\rho c_p)_{bf}+\phi(\rho c_p)_{np},$$
$$\frac{\rho_{nf}}{\rho_{bf}}=(1-\phi)+\phi\frac{\rho_{np}}{\rho_{bf}},$$
$$\frac{\sigma_{nf}}{\sigma_{bf}}=\left[1+\frac{3\left(\frac{\sigma_{np}}{\sigma_{bf}}-1\right)\phi}{\left(\frac{\sigma_{np}}{\sigma_{bf}}+2\right)-\left(\frac{\sigma_{np}}{\sigma_{bf}}-1\right)\phi}\right], \quad (8)$$
$$\frac{k_{nf}}{k_{bf}}=\left[\frac{(k_{np}+2k_{bf})-2\phi(k_{bf}-k_{np})}{(k_{np}+2k_{bf})+\phi(k_{bf}-k_{np})}\right]$$

Here, ϕ_s , d_n , h and s_p are represented solid volume fraction, radius, inter-particle distance and shape factor of nanoparticles. Also, the subscripts bf, np and nf represents basefluid, nanoparticle and nanofluid.

The dimensionless transformations of the mathematical model are:

$$u_1=a_1xf'(\zeta),\ v_1=a_1yg'(\zeta),\ w_1=-\sqrt{a_1\upsilon_{bf}}[f(\zeta)+g(\zeta)],$$
$$\zeta=\sqrt{\frac{a_1}{\upsilon_{bf}}}z,\ \theta(\zeta)=\frac{T-T_\infty}{T_w-T_0},\ \Phi(\zeta)=\frac{C-C_\infty}{C_w-C_0}$$

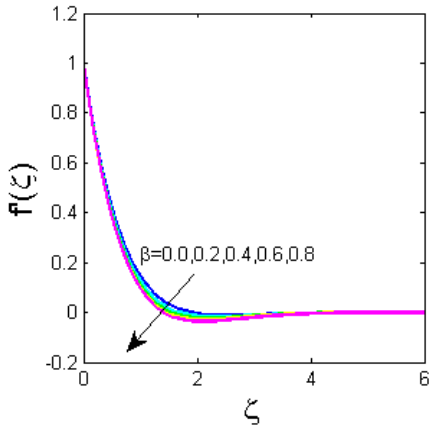

Fig. 1. f'(ζ) on β

By this transformation, Eqn (1) satisfies. While Eqns. (2) to (5) are :

$$f'''\left(\frac{1}{A_1A_2}-\beta(f+g)^2\right)-f'^2+2\beta f'f''(f+g)$$
$$+2\lambda E_1g'+(f+g)f''+2\beta E_1\lambda\left(g'^2-(f+g)g''-f'g'\right) \quad (9)$$
$$-\frac{A_4}{A_2}M\left(f'-\beta(f+g)f''\right)=0$$

$$g'''\left(\frac{1}{A_1A_2}-\beta(f+g)^2\right)-g'^2-2\beta(f+g)g'g''$$
$$+g''(f+g)-2\lambda E_2f'+2\lambda\beta E_2\left((f+g)f''-f'^2+f'g'\right) \quad (10)$$
$$+\frac{A_4}{A_2}M\left(\beta(f+g)g''-g'\right)=0$$

ISSN: 2366-1313

$$\theta''\left(\frac{A_5}{A_3\,\mathrm{Pr}}(1+\varepsilon\theta)-\Lambda_1(f+g)^2\right)+(f+g)(1+2\Lambda_1 f' -\Lambda_1(f'+g'))\theta'+(\Lambda_1(f+g)f''-f'-\Lambda_1 f'^2)(S_1+\theta) +\frac{A_5}{\mathrm{Pr}\,A_3}\varepsilon\theta'^2+\frac{H}{A_3}\theta=0 \tag{11}$$

$$\Phi''\left(\frac{1}{\mathrm{Sc}}-\Lambda_2(f+g)^2\right)+(f+g)(1-\Lambda_2(f'+g') +2\Lambda_2 f')\Phi'-\gamma\theta'\Phi'-(\Pi+\gamma\theta'')\Phi-(f'+\Lambda_2 f'^2 -\Lambda_2(f+g)f'')(S_2+\Phi)=0 \tag{12}$$

With corresponding boundary conditions are:

$$\begin{aligned}&\text{At } \zeta=0: \quad f'=1, \quad g'=S, \quad \theta=1-S_1, \quad \Phi=1-S_2\\ &\text{As } \zeta\to\infty: \quad f'\to 0, \quad g'\to 0, \quad \theta\to 0, \quad \Phi\to 0\end{aligned} \tag{13}$$

Where A_i's, i = 1, 2…5 in Eqs (9) - (12) shows the Thermophysical properties for the Maxwell nanofluid,

$$A_1=(1-\phi)^{2.5}, \quad A_2=\left(1-\phi+\phi\frac{\rho_{np}}{\rho_{bf}}\right),$$

$$A_3=\left(1-\phi+\phi\frac{(\rho c_p)_{np}}{(\rho c_p)_{bf}}\right),$$

$$A_4=\left[1+\frac{3\left(\frac{\sigma_{np}}{\sigma_{bf}}-1\right)\phi}{\left(\frac{\sigma_{np}}{\sigma_{bf}}+2\right)-\left(\frac{\sigma_{np}}{\sigma_{bf}}-1\right)\phi}\right],$$

$$A_5=\left[\frac{(k_{np}+2k_{bf})-2\phi(k_{bf}-k_{np})}{(k_{np}+2k_{bf})+\phi(k_{bf}-k_{np})}\right]$$

The parameters are defined here by $\beta = \lambda_1 a_1$ is Deborah relaxation number, $M = \sigma_{bf}B_0^2/\rho_{bf}a_1$ magnetic parameter, $\lambda = \omega/a_1$ rotation parameter, $\Lambda_1 = \lambda_2 a_1$ thermal relaxation, $\lambda_2 = \lambda_3 a_1$ concentration relaxation, $H=H_0/(\rho c_p)_{bf}a_1$ heat generation, $S=a_2/a_1$ stretching ratio, $Sc=\upsilon_{bf}/D_A$ Schmidt number, ε variable thermal conductivity, $Pr=\upsilon_{bf}(\rho c_p)_{bf}/k_{bf}$ Prandtl number, $\gamma = k^*(T_w-T_\infty)/T_r$, thermophoretic velocity, $\Pi=\Gamma/a_1$ chemical reaction, $S_1=e_1/d_1$ thermal stratification and $S_2=e_2/d_2$ solutal stratification.

Table 2. Comparison of f' (0) and g' (0) with previous result when β = 0.3 and α = 0.5

M	Anber Saleem [1]		Current result	
	f''(0)	g''(0)	f''(0)	g''(0)
0.0	1.22476	0.519446	1.224759	0.519444
0.2	1.24294	0.530167	1.242939	0.530167
0.4	1.29612	0.561217	1.296116	0.561218
0.6	1.38067	0.609718	1.380666	0.609718
0.8	1.49161	0.672063	1.491606	0.672063
1.0	1.62371	0.744855	1.623710	0.744855

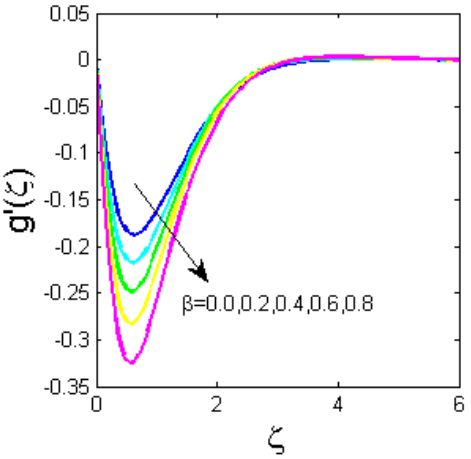

Fig. 2. g'(ζ) on β

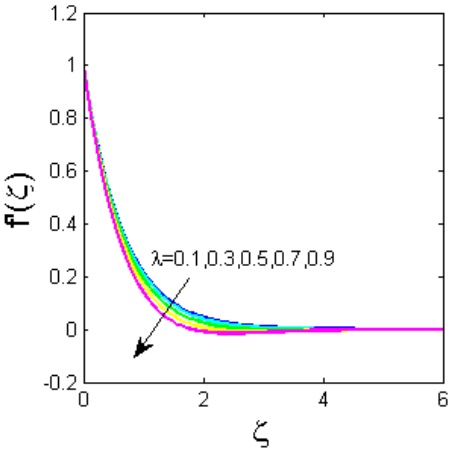

Fig. 3. f'(ζ) on λ

3. MATHEMATICAL SOLUTION

By changing the ODE Equations (9) - (12) as an initial value problem with boundary conditions, we want to: $f=G_1$, $f'=G_2$, $f''=G_3$, $g=G_4$, $g'=G_5$, $g''=G_6$, $\theta=G_7$, $\theta'=G_8$, $\Phi=G_9$, $\Phi''=G_{10}$ and then, we obtain systematic first-order equation then it solve through bvp4c Matlab solver.

4. DISCUSSION OF THE FINDINGS

Maxwell nanofluid over a bidirectional sheet due to rotating frame with thermophoresis velocity, variable thermal conductivity and double stratification solved numerically and graphically. Table 1 represents Thermophysical properties of nanofluids. Moreover Magnetite nanoliquid is

ISSN: 2366-1313

used throughout the solvable graphical solution. Table 2 represents comparison result of various Magnetic field by previous article and good agreement with both the results. While rising of rotation strength, thermal conductivity and shape factor, temperature reduces in a moving fluid in Table 3.

Table 3. Numerical results over $-\theta'(0)$

λ	ε	s_p	$-\theta'(0)$
0.1	0.1	3.0	0.768524
0.5			0.626028
1.0			0.520531
2.0			0.428470
0.2	0.1		0.746036
	0.5		0.583756
	1.0		0.465347
	2.0		0.340953
	0.1	3.7	0.735140
		4.9	0.719094
		5.7	0.709895
		8.9	0.681524

This described that in industry application, nanofluid flow of rotating metal sheet with high resistance and different shapes gives low temperature due to Coriolis force. Table 4. remains rising of thermophoresis force, energy also rises.

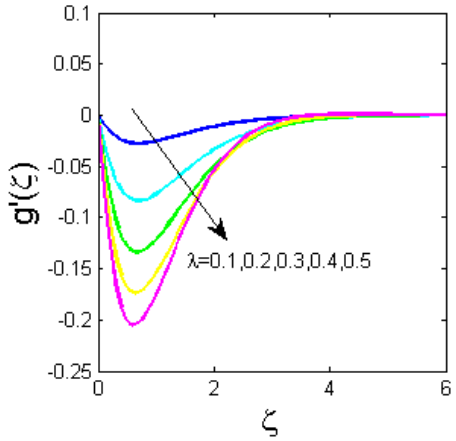

Fig. 4. g′(ζ) on λ

The Deborah number increases slowly, then the waves of velocity reduces. Especially in g'(ζ) leads to negative direction. This means that enhancement of viscous force in fluid turns to reduce the speed of fluid flow in Figure. 1 and 2. By stretching the surface in both direction, the viscosity goes stronger then velocity decreases. By amplifying rotation rate gradually the velocity field diminishes in both the axes. But in y-direction, the velocity reduces to negative direction then increases monotonically to converge to zero. While rotating the frame, fluid moves thoroughly so fluid velocity runs slowly noted in Figure. 3 and 4. In thermal field, rising of rotating strength gives high temperature. By increasing the rotation of stretched sheet, there will be more force act as a heat transfer and it increases the temperature which shows in Figure. 5.

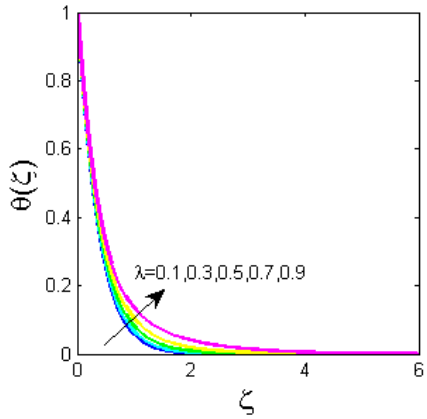

Fig. 5. θ(ζ) on λ

Here introduced the various shape and its factor of nanoparticle in fluid. Considering the different shapes, thermal conductivity improves its nature in nanoliquid. Figure. 6 shows that in blade shape, temperature is maximum and lowest in spherical shape nanoparticles. For larger values of thermal conductivity, the heat transfer increases its rate noticed in Figure. 7.

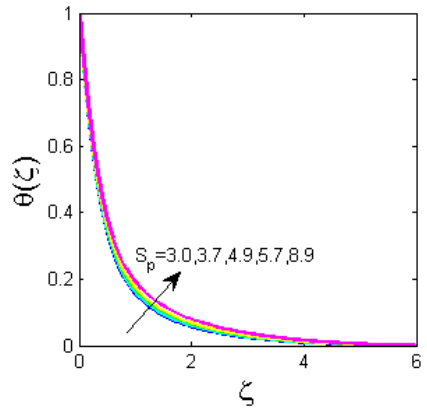

Fig. 6. θ(ζ) on s_p

ISSN: 2366-1313

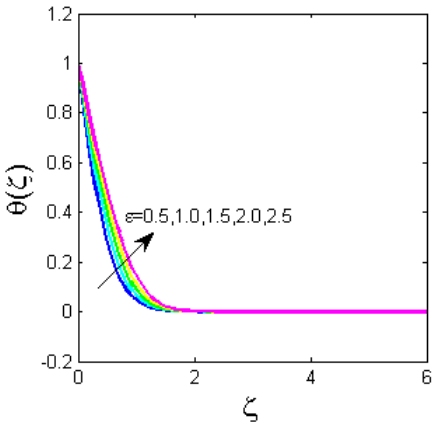

Fig. 7. θ(ζ) on ε

Increasing of variable thermal conductivity in moving metal sheet, it raises the temperature of fluid. The enhancement of thermophoresis parameter decreases concentration sketch in Figure. 8. If γ <1, concentration field scattered but for γ >1, solute field decreases gradually. Figure. 9 displays that increasing of thermal stratification reduces the temperature of fluid flow. This means that stratifying stretched sheet with all the other parameters remains constant then automatically temperature decreases. In solute field, stratification parameter increases concentration profile decreases in Figure. 10. By stratified condition nanoparticles arranged in a different layer then there is non-zero viscosity occurs. It leads concentration to decay.

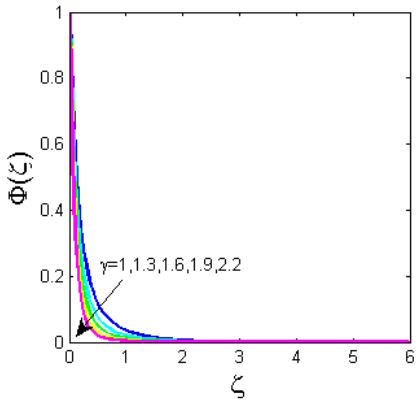

Fig. 8. Φ (ζ) on γ

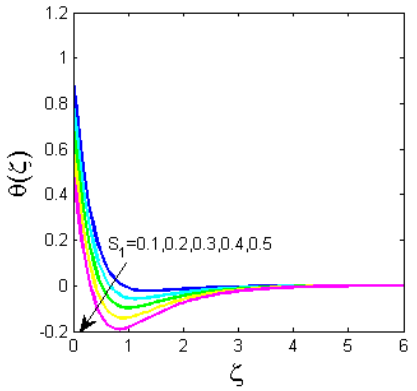

Fig. 9. θ(ζ) on S_1

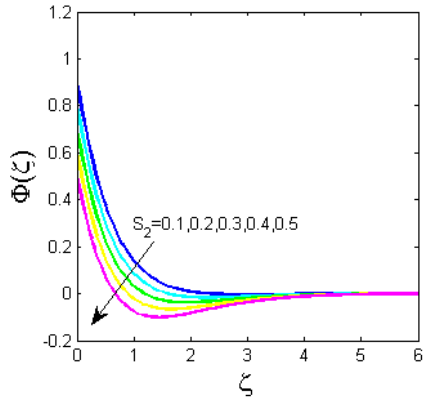

Fig. 10. Φ (ζ) on S_2

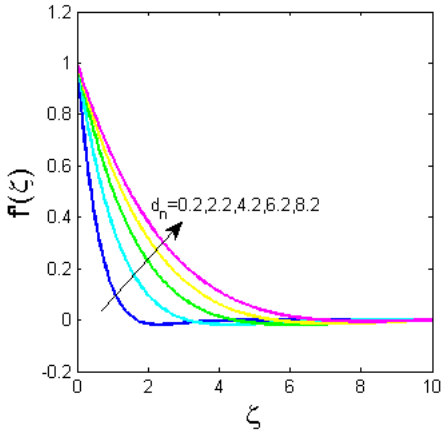

Fig. 11. f′(ζ) on d_n

Figure. 11 and 12 explains amplifying the diameter of nanoparticle over the velocities f'(ζ) and g'(ζ). When the diameter of nanoparticles increases then magnitude of the velocity increases in both direction but in y-direction after certain point the velocity decreases monotonically.

ISSN: 2366-1313

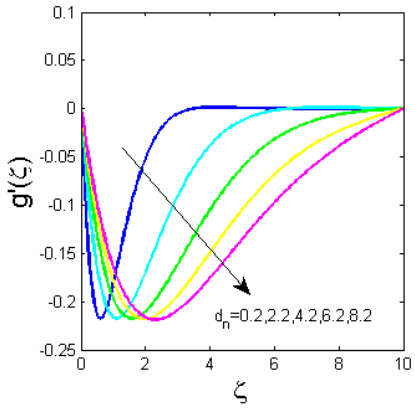

Fig. 12. g'(ζ) on d_n

Rising of diameter in nanoparticle rises the fluid also because of enlarging the particle size. By enhancing nanoparticle volume fraction in velocities and temperature field in Figure, 13, 14 and 15. The velocity f'(ζ) in x-direction diminishes when increasing of nanoliquid volume fraction. This indicates that motion of the fluid retarded when the nanoparticles collides.

Boundary layer thinner for larger values of ϕ_s. In y-direction, magnitude of velocity increases with nanoparticle. The enhancement of solute nanoparticles enhances the fluid flow temperature. The collision of nanoparticle increases then concentration field also rises. With this collisions and causing of heat transfer, temperature increases and also improves the thermal conductance.

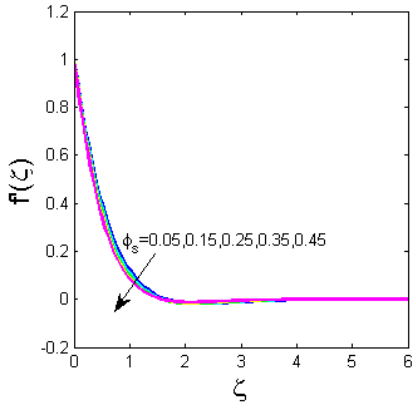

Fig. 13. f'(ζ) on ϕ_s

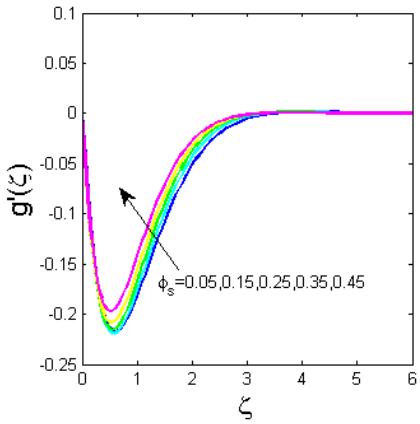

Fig. 14. g'(ζ) on ϕ_s

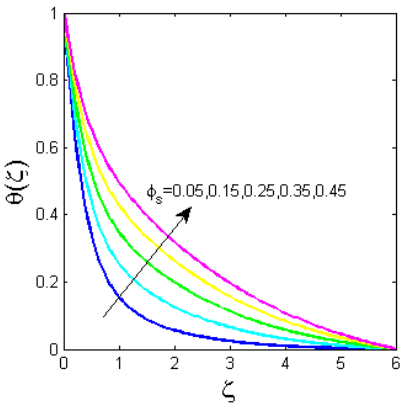

Fig. 15. θ(ζ) on ϕ_s

5. CONCLUSION

Maxwell nanoliquid with double stratification, thermophoresis velocity and variable thermal conductivity of bidirectional rotating surface illustrated. This model is solved numerically and graphically through bvp4c numerical Matlab solver. Finally the results of findings are:

- For rising of elasticity parameter, viscosity increases in fluid then velocity reduces its nature.
- Moreover, boundary layer thickness of velocity becomes thinner but increasing the diameter of nanoparticle and volume fraction, boundary layer enhances.
- The temperature is more effective in blade shape nanoparticle but vice-versa in spherical shape factor.
- Due to collision of nanoparticle, temperature strengthens and also it proves thermal conductivity.
- Thermal boundary layer becomes stronger in temperature field.

ISSN: 2366-1313

- Stronger variable thermal conductivity gives high temperature profile.
- Larger thermophoresis velocity becomes weaker concentration field.

Table 4. Numerical results of $-\Phi'(0)$

λ	γ	Sc	$-\Phi'(0)$
0.1	1.0	1.0	1.020710
0.5			0.865282
1.0			0.734294
2.0			0.614273
0.2	1.0		0.997691
	1.3		1.034150
	1.7		1.083632
	2.1		1.133968
		1.5	1.340849
		2.0	1.641802
		2.5	1.911508
		3.0	2.158553

REFERENCES

[1] Ahmad, Shafiq and Khan, Muhammad Naveed and Nadeem, Sohail. "Mathematical analysis of heat and mass transfer in a Maxwell fluid with double stratification." *Physica Scripta* 96.2 (2020).

[2] Ahmadian, Ali and Bilal, Muhammad and Khan, Muhammad Altaf and Asjad, Muhammad Imran. "The non-Newtonian maxwell nanofluid flow between two parallel rotating disks under the effects of magnetic field." *Scientific Reports* 10.1 (2020): 1--14.

[3] Akbar, Asia Ali and Ahammad, N Ameer and Awan, Aziz Ullah and Hussein, Ahmed Kadhim and Gamaoun, Fehmi and Tag-ElDin, ElSayed M and Ali, Bagh. "Insight into the role of nanoparticles shape factors and diameter on the dynamics of rotating water-based fluid." *Nanomaterials* 12.16 (2022): 2801.

[4] Ashraf, Muhammad and Abbas, Amir and Ali, Aamir and Shah, Zahir and Alrabaiah, Hussam and Bonyah, Ebenezer. "Numerical simulation of the combined effects of thermophoretic motion and variable thermal conductivity on free convection heat transfer." *AIP Advances* 10.8 (2020): 085005.

[5] Bandaru, Mallikarjuna and Vijaya, R Bhuvana. "Effect of variable thermal conductivity on convective heat and mass transfer over a vertical plate in a rotating system with variable porosity regime." *Journal of Naval Architecture and Marine Engineering* 11.1 (2014): 83-92.

[6] Ewis, Karem Mahmoud. "Effects of Variable Thermal Conductivity and Grashof Number on Non-Darcian Natural Convection Flow of Viscoelastic Fluids with Non Linear Radiation and Dissipations." *Journal of Advanced Research in Applied Sciences and Engineering Technology* 22.1 (2021): 69--80.

[7] Gbadeyan, JA and Titiloye, EO and Adeosun, AT. "Effect of variable thermal conductivity and viscosity on Casson nanofluid flow with convective heating and velocity slip." *Heliyon* 6.1 (2020).

[8] Hazarika, GC and Jadav, Konch. "Effects of Variable viscosity and thermal conductivity on MHD free convective flow along a vertical porous plate with viscous dissipation." *International Journal of Mathematics Trends and Technology* 15.1 (2014): 70--85.

[9] Mabood, F and Rauf, A and Prasannakumara, BC and Izadi, M and Shehzad, SA. "Impacts of Stefan blowing and mass convention on flow of Maxwell nanofluid of variable thermal conductivity about a rotating disk." *Chinese Journal of Physics* 71 (2021): 260--272.

[10] Mustafa, M and Hayat, T and Alsaedi, A. "Rotating flow of Maxwell fluid with variable thermal conductivity: an application to non-Fourier heat flux theory." *International Journal of Heat and Mass Transfer* 106 (2017): 142--148.

[11] Nabwey, Hossam A and Rashad, Ahmed M and Mahdy, Abd El Nasser and Shaaban, Shaaban M. "Thermal Conductivity and Thermophoretic Impacts of Micropolar Fluid Flow by a Horizontal Absorbent Isothermal Porous Wall with Heat Source/Sink." *Mathematics* 10.9 (2022): 1514.

[12] Ramzan, Muhammad and Gul, Hina and Mursaleen, M and Nisar, Kottakkaran Sooppy and Jamshed, Wasim and Muhammad, Taseer. "Von Karman rotating nanofluid flow with modified Fourier law and variable characteristics in liquid and gas scenarios." *Scientific Reports* 11.1 (2021): 1--17.

[13] Reddy, M Gnaneswara. "Effects of Thermophoresis, viscous dissipation and Joule heating on steady MHD flow over an

ISSN: 2366-1313

inclined radiative isothermal permeable surface with variable thermal conductivity." *Journal of Applied Fluid Mechanics* 7.1 (2014): 51--61.

[14] Shehzad, SA and Qasim, M and Alsaedi, A and Hayat, T and Alsaadi, F. "Radiative Maxwell fluid flow with variable thermal conductivity due to a stretching surface in a porous medium." *Journal of Aerospace Engineering* 27.5 (2014).

[15] Srinivasacharya, Darbhasayanam and Mallikarjuna, Bandaru and Bhuvanavijaya, Rachamalla. "Effects of thermophoresis and variable properties on mixed convection along a vertical wavy surface in a fluid saturated porous medium." *Alexandria Engineering Journal* 55.2 (2016): 1243--1253.

[16] Tarakaramu, Nainaru and Narayana, PV Satya and Venkateswarlu, Bhumarapu. "Numerical simulation of variable thermal conductivity on 3D flow of nanofluid over a stretching sheet." *Nonlinear Engineering* 9.1 (2020): 233--243.